INDIAN JOURNAL OF SCIENCE AND TECHNOLOGY

RESEARCH ARTICLE

Microstructural Effect and FTIR Study of Co-Doped Calcium Copper Titanate ($CaCu_3Ti_4O_{12}$)

Sachin Tripathi[1]*, Seema Srivastava[1], Ameer Azam[2], Upendra Kumar Mishra[3,4]

1 Department of Physics,, Integral University, Lucknow, 226026, India
2 Department of Physics, Faculty of Science, Islamic University of Madinah Al Jamiah, Madinah, 42351, Saudi Arabia
3 Department of Applied Science, Shri Ramswaroop Memorial College of Engineering and Management, Lucknow, 226028, India
4 Dr. A.P.J. Abdul Kalam Technical University, Lucknow, 226031, India

OPEN ACCESS

Received: 23-07-2024

Accepted: 01-08-2024

Published: 21-08-2024

Citation: Tripathi S, Srivastava S, Azam A, Mishra UK (2024) Microstructural Effect and FTIR Study of Co-Doped Calcium Copper Titanate ($CaCu_3Ti_4O_{12}$). Indian Journal of Science and Technology 17(33): 3467-3472. https://doi.org/10.17485/IJST/v17i33.2369

* **Corresponding author**.

sachhintripathi@gmail.com

Funding: None

Competing Interests: None

Published By Indian Society for Education and Environment (iSee)

ISSN
Print: 0974-6846
Electronic: 0974-5645

Abstract

Objectives: To discover the influence of the Co atom by replacing the Ti atom in CCTO on its chemical properties. **Methods:** Pure and Co-doped CCTO ($CaCu_3Ti_{4-x}Co_xO_{12}$, x=0.05, 0.10, 0.15) ceramics synthesized via solid-state reaction and heating at 950°C for 12 hours with a heating rate of 4°C/min. X-ray Diffraction (XRD) confirmed that CCTO has a single-phase structure. Field Effect Scanning Electron Microscopy (FE-SEM) was used to examine the grain size, and Fourier Transform Infrared Spectroscopy (FT-IR) was used to record the absorption band for all samples. **Findings:** The size of the material decreases by the doping of the Co atom. No change observed in the shape by the doping of Co atoms in place of Ti atoms. The average particle size of the samples is between 0.3-0.5 micrometers. **Novelty:** The bond strength improves with the doping of the Cobalt atom. A broad absorption band is observed with the peak of this band shifting towards lower wave numbers. This will be a required condition for energy storage applications. It also enhances the use of CCTO in pharmaceuticals, chemical synthesis, and environmental remediation.

Keywords: FESEM; XRD; FTIR; EDS; CCTO

1 Introduction

The demand for electronics is increasing, and energy-related problems are becoming a global issue as science and technology advance[(1)]. Titanium dioxide (TiO_2), barium titanate ($BaTiO_3$), strontium titanate ($SrTiO_3$), and calcium copper titanate ($CaCu_3Ti_4O_{12}$/CCTO) are key materials that are widely used in electrical applications[(2–5)]. Although significant progress has been made in developing these dielectric materials, the main challenges still include low energy storage density and high electron loss.

The substrate, known as a photocatalyst, is an essential component of the photocatalysis process, which uses light to speed up chemical reactions and remove pollutants

from the environment[6]. The nano-catalyst derived from calcium copper titanate, obtained from mineral industry waste, has shown promising results in reducing pollution problems and increasing energy efficiency[7]. Its ability to efficiently adsorb a wide range of contaminants, such as heavy metal ions, dyes, and organic molecules, makes calcium copper titanate an effective and versatile tool for water pollutant removal. Growing populations and accelerated industrialization have pushed scientists to look for green solutions to the pollution problem that use renewable energy sources like visible light. Pollutants and pharmaceutical waste can only decompose when exposed to UV light, which shares very small of its wavelengths with visible light[8]. TiO_2 is well known photo-catalytic in UV radiation and it belongs to the family of perovskite ABO_3 structure. CCTO perovskite shows good photo-catalytic performance in water pollutants and pharmaceutical waste. Photo-catalysis has gained a lot of interest due to its lower cost, increased capacity, and environmentally safe and green methods[9]. In the present study, the doping of metal transition Cobalt (Co) atoms in pure CCTO has been done to enhance its photo-catalytic properties.

In this study, the abbreviations CCTO and CCTCoO are used to refer to undoped $CaCu_3Ti_4O_{12}$ and $CaCu_3Ti_{4-x}Co_xO_{12}$(x = 0.05, 0.10, 0.15), respectively. These materials were prepared using the solid-state reaction method. To determine their properties, X-ray diffraction (XRD), energy dispersive X-ray spectroscopy (EDS), Field effect scanning electron microscopy (FE-SEM), and Fourier transform infrared spectroscopy (FTIR) were utilized to analyze their microstructure, size, and absorption bands.

2 Methodology

The raw materials $CaCO_3$ (Thomas Baker, purity>99%), CuO (Thomas Baker, AR grade), TiO_2 (Sigma Aldrich, purity>99.9%), and Co_3O_4 (Sigma Aldrich, purity>99.5%) were used for synthesis of pure ($CaCu_3Ti_4O_{12}$) and Co-doped calcium copper titanate ($CaCu_3Ti_{4-x}Co_xO_{12}$). Precursors are mixed by using an agate mortar. The mixture was then dried for 2 hours. Following this, the powder was calcined at 950°C for 12 hours in a programmable furnace with a heating rate of 4°C per minute.

$$CaCO_3 + 3CuO + 4TiO_2 \xrightarrow{950^\circ C} CaCu_3Ti_4O_{12} + CO_2 \uparrow$$

To synthesize cobalt-doped CCTO ($CaCu_3Ti_{4-x}Co_xO_{12}$), we used cobalt oxide (Co_3O_4, Sigma Aldrich, Purity>99.5%). Similarly, a solid-state reaction process was used to synthesize all of the cobalt-doped CCTO (CCTCoO), with varying doping concentrations of 5%, 10%, and 15%.

$$CaCO_3 + 3CuO + (4-x)TiO_2 + xCo_3O_4 \xrightarrow{950^\circ C} CaCu_3Ti_{4-x}Co_xO_{12}$$

The XRD pattern of all precursors was confirmed by PANalytical X-ray Diffractometer (40kV, 30 mA). The pattern recorded with Cu-K_α (λ=1.54 Å) in the 2θ range of 20° to 80°. FESEM is used to study the morphology and microstructure of CCTO. The study of chemical bonding has been done by using FT-IR spectroscopy.

3 Results and Discussion

3.1 X-ray Diffraction

The XRD pattern of pure and cobalt-doped CCTO has been shown in Figure 1. The introduction of doped ions into the CCTO lattice is almost linked to the diffraction peak shift. The XRD pattern of 5% Co and 15% Co doped shows a distinct shift to lower angles of diffraction (220) peak, which is likely caused by the larger bivalent Co ionic radius[10] which found that cobalt existing in +2 and +3 states can occupy Cu^{2+} and Ti^{4+} as separate, depending on its oxidation state. Based on the different ionic radius ($r(Co^{2+})$ = 0.75 Å, $r(Co^{3+})$ = 0.55 Å, $r(Cu^{2+})$ = 0.57 Å, and $r(Ti^{4+})$ = 0.61 Å), this is consistent with it. Ti ion substitution by a smaller trivalent Co ionic radius is the primary reason for the comparatively mild shift to higher angles in 10% doped CCTO. The lattice parameters were calculated to be 7.389, 7.409, 7.387, and 7.386 Å, respectively. The variation in the lattice parameters shows good agreement with the shift tendency of the diffraction (220) peak that is due to the atomic radius differences. Research suggests that Co^{3+} ions are more suitable for occupying Ti sites than Cu sites in CCTO[11]. The CCTO structure was confirmed using X-ray diffraction (XRD, PAN analytical) with Cu Kα (λ = 1.5406 Å).

The size of the crystallites in the samples appears to decrease with an increase in the amount of Co doping. Figure 2 shows the crystallite size from the W-H plot, Debye–Scherrer, and Modified Scherrer equation. It is also essential to acknowledge that other factors, such as sample preparation and processing techniques, may also affect the properties of material.

Table 1. Lattice parameter of pure and Co doped samples

S.No.	Sample name	Lattice parameter (Å)
1.	$CaCu_3Ti_4O_{12}$	7.389
2.	$CaCu_3Ti_{3.95}Co_{0.05}O_{12}$	7.3892
3.	$CaCu_3Ti_{3.90}Co_{0.10}O_{12}$	7.3878
4.	$CaCu_3Ti_{3.85}Co_{0.15}O_{12}$	7.3894

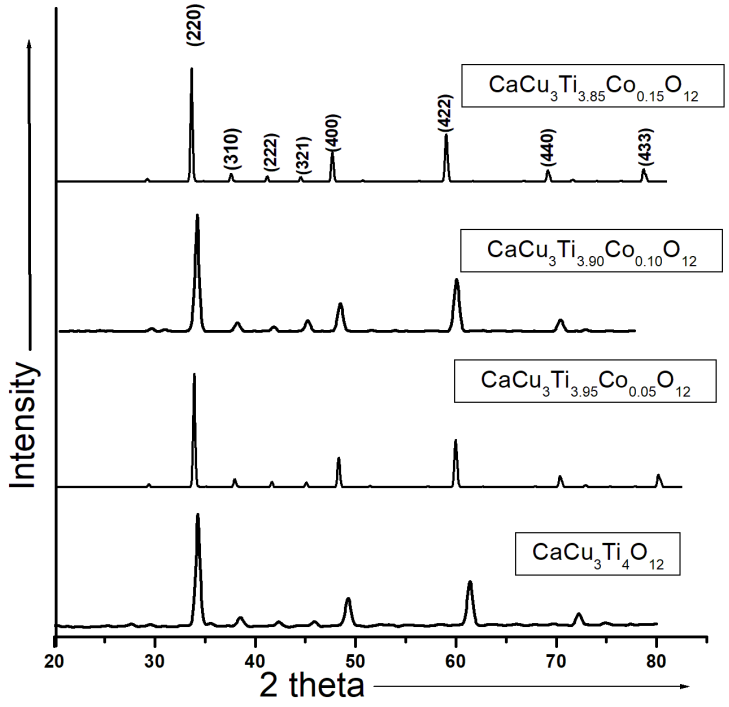

Fig 1. XRD pattern of pure CCTO and co-doped CCTO at x= 5%, 10%, and 15%

Table 2. Crystallite size, micro-strain, and dislocation density by Williamson-Hall plot

Samples	Calcination (°C)	Williamson Hall plot size (in nm)	Dislocation Density (δ)	Debye–Scherrer equation size (in nm)	Modified Scherrer equation size (in nm)
$CaCu_3Ti_4O_{12}$		48.1117608	0.043201368	31.5103124	37.11315371
$CaCu_3Ti_{3.95}Co_{0.05}O_{12}$	950°C	30.17008333	0.109861868	24.30685709	26.76865074
$CaCu_3Ti_{3.90}Co_{0.10}O_{12}$		15.47183761	0.417749754	15.67114674	15.35439042
$CaCu_3Ti_{3.85}Co_{0.15}O_{12}$		44.28636086	0.050987065	31.15267611	35.88902198

3.2 FE-SEM (Field Effect Scanning Electron Microscopy Analysis

The FE-SEM images of pure and Co-doped calcium copper titanate have been shown in Figure 2. The grains of the material are uniformly formed, with an average size of 1.0-1.3 micrometers, although smaller grains measuring 0.4-0.6 micrometers are present[12]. Interestingly, the cubic shape of the material remains unchanged even when cobalt is doped at various concentrations. This suggests that the doping process does not significantly affect the overall shape of the material. For instance, increasing the concentration of cobalt by 10% could potentially result in a more pronounced change in the shape of the material[13]. In the cobalt doping, it is seen that the average grain size of the sample lies between 0.3-0.5μm. The smaller grain has to be found about 200 nm in the doping of 15% cobalt. The 15% has been shown lesser grain size as compared to other doping concentrations.

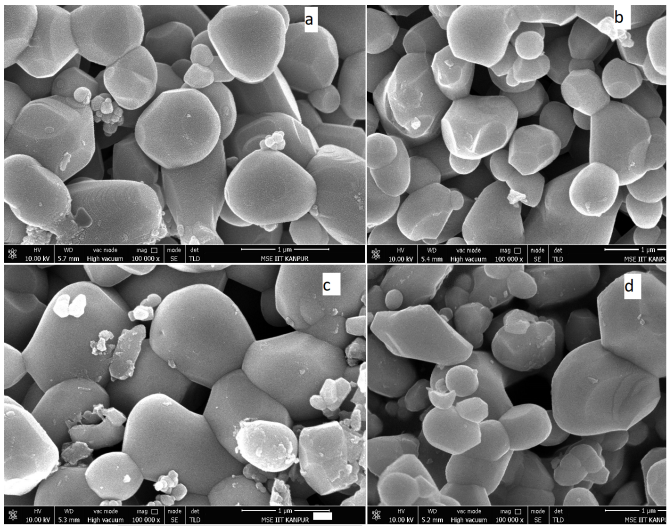

Fig 2. FE-SEM images of (a) pure CCTO and Co-doped (b) 5%, (c) 10%, (d) 15% CCTO

3.3 EDS (Energy Dispersive Spectra)

EDS gives the stoichiometric number of used precursors. EDS analysis is commonly utilized to examine the presence of elements in CCTO and to determine the weight percent of each element. Additionally, this technique reveals the varying concentrations of Co doping in both pure CCTO and the doped ceramics. When conducting EDS analysis, multiple regions of both pure and doped ceramics are focused and the results are displayed in Figure 3. In the same manner weight % of each element is seen for all samples. The presence of the carbon element is evident due to the sample being deposited on a carbon tape, resulting in a negligible weight for this element. The EDS spectra provide information on the Ca, Cu, and Ti elements in the pure ceramic and the weight percent of Co with Ca, Cu, and Ti in the doped samples [14]. The weights of Ca, Cu, and Ti were 6.15, 24.63, and 62.55, respectively for pure CCTO, while the atomic percentages were also provided for all elements in the synthesized powder samples. The EDS observations partially support the idea of Co replacing Ti at specific sites. The smallest grain size and thinnest intergranular phase, which may be related to the dielectric and electrical properties, are processed by 5% Co-doped CCTO. It is concluded that the co-doping causes a change in the grain size and the geometric form of the intergranular phase (related to the mechanical properties of the material).

3.4 FTIR Spectroscopy

Figure 4 shows the FT-IR spectra of all the synthesized samples. The Ti-O-Ti peak present at 460cm^{-1} wave number is indicative of strong chemical bonding between titanium and oxygen atoms in the material. This bond is a characteristic feature of titanium oxide and is responsible for its optical and electronic properties. This strong chemical bonding is likely due to the synthesis process of material at high temperatures, which promotes the formation of a TiO_6 crystalline structure. The peak at 570 cm^{-1} corresponds to the vibrations of the Co-O bond, confirming the successful incorporation of cobalt ions into the calcium-copper titanate crystal structure. The intensity of this peak increased with increased cobalt concentration, suggesting that more cobalt ions are being incorporated into the lattice [15]. Additionally, the broadening of this peak suggests an increase in disorder and distortion of the crystal structure due to the substitution of larger cobalt ions for smaller titanium ions [16]. The presence of the 620 cm^{-1} peak indicates the vibration of Cu-O bonds, which can be attributed to the copper oxide component in the material. The FTIR data provides evidence of the successful doping of cobalt into the calcium copper titanate structure and the formation of the desired crystal phases.

The CCTO structure displays the TiO_6 absorption band within the 380-700 cm-1 range. The O-H bond peaks shift leftward, indicating enhanced bond stability [17]. The peak shifting indicates energy storage applications. The large absorption band gives the enhancement of photocatalytic activity. Co-doping CCTO with 10% Co increases stability and, thereby can used for the photocatalytic activity of CCTO. Additionally, the small size of CCTO nanoparticles enhances their efficiency in degrading organic compounds under UV light. This will help in the field of pharmaceutical waste management and water pollutants [18,19].

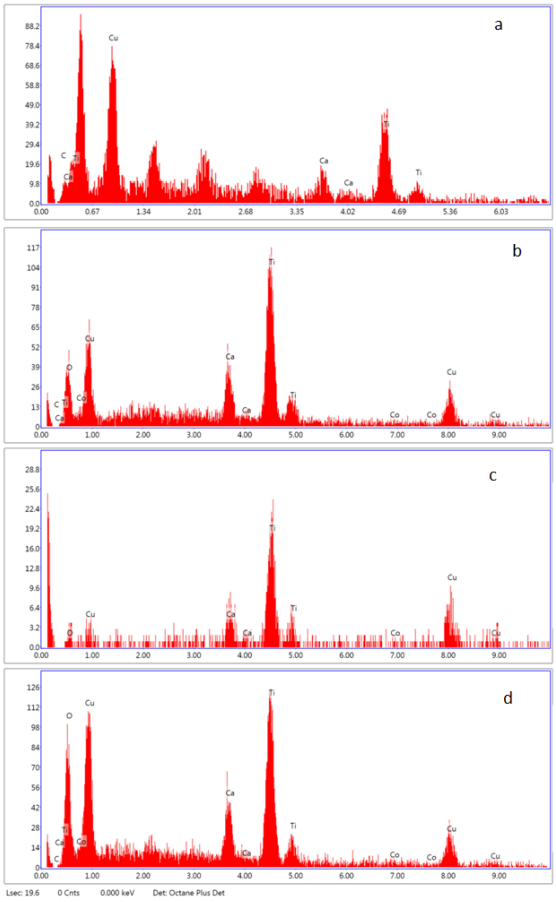

Element	Weight %	Atomic %
C K	6.68	23.13
Cu L	24.63	16.13
Ca K	6.15	6.39
Ti K	62.55	54.35

Element	Weight %	Atomic %
C K	2.67	7.63
O K	17.06	36.55
Co L	0.60	0.35
Cu L	17.09	9.22
Ca K	10.59	9.05
Ti K	51.99	37.20

Element	Weight %	Atomic %
C K	17.00	39.92
O K	9.10	16.04
Co L	0.93	0.45
Cu L	4.51	2.00
Ca K	11.01	7.75
Ti K	57.44	33.83

Element	Weight %	Atomic %
C K	1.89	5.16
O K	22.44	45.97
Co L	0.72	0.40
Cu L	24.15	12.45
Ca K	9.34	7.64
Ti K	41.46	28.37

Fig 3. EDS images of (a) pure CCTO and Co-doped (b) 5%, (c) 10%, (d) 15% CCTO

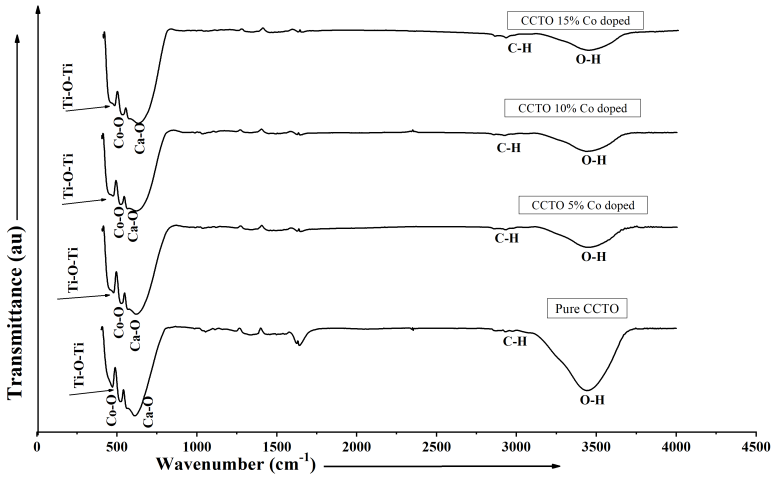

Fig 4. FTIR spectra of Pure and Co-doped CCTO

4 Conclusion

Pure and Co-doped samples were prepared by the solid-state reaction method to provide structural information about the samples. The XRD patterns of all the samples clearly show that the peaks are shifted towards a lower angle. The crystal structure was decreased by the doping of Co atom due to the difference in ionic radii of Co and Ti. FESEM gives smaller grain sizes of up to 0.3-0.5μm. The particle size is about 200 nm by the doping of 15% Co. FT-IR analysis shows the stretching of the O-H bond towards a lower wave number. Therefore, it is used for energy storage applications. This will enhance the photocatalytic activity of the samples. In future applications, Co-doped CCTO can be used as organic compounds under UV light and have significant implications for various industries such as pharmaceuticals and environmental remediation of water pollutants.

Acknowledgment

Authors are thankful to the Research and Development of Integral University, Lucknow for providing the research facilities and manuscript communication number IU/R&D/2024-MCN0002872.

References

1) Jayakrishnan AR, Silva J, Kamakshi K, Dastan D, Annapureddy V, Pereira M, et al. Are lead-free relaxor ferroelectric materials the most promising candidates for energy storage capacitors? *Progress in Materials Science*. 2023;132:1–33. Available from: https://doi.org/10.1016/j.pmatsci.2022.101046.
2) Parangi T, Mishra MK. Titanium Dioxide as Energy Storage Material: A Review on Recent Advancement. *IntechOpen*. 2021. Available from: http://dx.doi.org/10.5772/intechopen.99254.
3) Sun J, Yan G, Fang B, Zhao X, Zhang S, Lu X, et al. Improving energy storage performance of barium titanate-based ceramics by doping MnO2. *Journal of Energy Storage*. 2024;78. Available from: https://doi.org/10.1016/j.est.2023.110007.
4) Liu L, Liu Y, Hoa J, Chen J, Li P, Chen S, et al. Multi-scale collaborative optimization of SrTiO3-based energy storage ceramics with high performance and excellent stability. *Nano Energy*. 2023;109. Available from: https://doi.org/10.1016/j.nanoen.2023.108275.
5) Kawrani S, Boulos M, Cornu D, Bechelany M. From Synthesis to Applications: Copper Calcium Titanate(CCTO) and its Magnetic and Photocatalytic Properties. *Chemistry open*. 2019;8:922–950. Available from: https://doi.org/10.1002/open.201900133.
6) Saravanan A, Kumar PS, Jeevanantham S, Anubha M, Jayashree S. Degradation of toxic agrochemicals and pharmaceutical pollutants: Effective and alternative approaches toward photocatalysis. *Environ Pollut*. 2022;298. Available from: https://doi.org/10.1016/j.envpol.2022.118844.
7) Makhoul E, Boulos M, Cretin M, Lesage G, Miele P, Cornu D, et al. *Nanomaterials*. 2023;2119(14):13–13. Available from: https://doi.org/10.3390/nano13142119.
8) Kushwaha HS, Madhar NA, Ilahi B, Thomas P, Halder A, Vaish R. Efficient Solar Energy Conversion Using CaCu3Ti4O12 Photoanode for Photocatalysis and Photoelectrocatalysis. *Scentific Reports*. 2016;1(6). Available from: https://doi.org/10.1038/srep18557.
9) Alam N, Khatoon T, Chandel VS, Azam A. Band Gap Engineering in Zinc Doped Sodium Hexa-titanate. *Indian Journal of Science and Technology*. 2019;12(21). Available from: https://doi.org/10.17485/ijst/2019/v12i21/143934.
10) Wang J, Lu Z, Deng T, Zhong C, Chen Z. Improved dielectric, nonlinear and magnetic properties of cobalt-doped CaCu3Ti4O12 ceramics. *Journal of the European Ceramic Society*;2018:1–7. Available from: https://sci-hub.se/10.1016/j.jeurceramsoc.2018.04.015.
11) Zhuk NA, Lutoev VP, Lysyuk AY, Makeev BA, Belyy VA, Nekipelov SV, et al. Thermal behavior, magnetic properties, ESR, XPS, Mössbauer and NEXAFS study of Fe-doped CaCu3Ti4O12 ceramics. *Journal of Alloys and Compounds*. 2021;855(1). Available from: https://doi.org/10.1016/j.jallcom.2020.157400.
12) Kumari N, Meena S, Rathore D, Singhal R, Dwivedi UK. Study of dielectric properties of CaCu3Ti4O12 synthesized via different routes: Effect of sintering temperature. *Ceramics International*. 2023;49(2):2549–2556. Available from: https://doi.org/10.1016/j.ceramint.2022.09.234.
13) Kumar P, Pathak S, Singh A, Kuldeep, Khanduri H, Wang X, et al. Optimization of cobalt concentration for improved magnetic characteristics and stability of CoxFe3-xO4 mixed ferrite nanomagnetic fluids. *Materials Chemistry and Physics*. 2021. Available from: https://doi.org/10.1016/j.matchemphys.2021.124476.
14) Renzhong X, Yuanqing C, Tao L, Dewei L, Siyuan C, Hongxuan C, et al. Effects of Lu Doping on Microstructures and Electrical Properties of CaCu3Ti4O12 Ceramics. *Journal of Superconductivity and Novel Magnetism*. 2021;34:1–13. Available from: https://doi.org/10.1007/s10948-021-05978-9.
15) Maini A, Shah MA. Investigation on physical properties of nanosized copper oxide (CuO) doped with cobalt (Co): A material for electronic device application. *International Journal of Ceramic Engineering & Science*. 2021;p. 192–199. Available from: https://doi.org/10.1002/ces2.10097.
16) Dey A, Rasane P, Kaur S, Singh J, Luwang. Tofu: technological and nutritional potential. *Indian Food Industry Mag* . 2017;36:8–24. Available from: https://www.researchgate.net/publication/323676422_Tofu_technological_and_nutritional_potential.
17) Alam N, Khatoon T, Chandel VS, Azam A, Rashmi. Comparative Analysis of Sodium Hexa-titanate (Na2Ti6O13) & Sodium-Potassium Hexa-titanate (Na1.5K0.5Ti6O13). . *International Conference on Multifunctional Materials*. 2020. Available from: https://doi.org/10.1088/1742-6596/1495/1/012034.
18) Khatoon T, Alam N, Chandel VS, Azam A, Srivastava S, Gupta J. Exploring the synergistic effects of La3+ substitution on dielectric performance of manganese cobalt ferrite: Implications for advanced electronic applications. *Ceramics International*. 2024;50(4):7156–7167. Available from: https://doi.org/10.1016/j.ceramint.2023.12.083.
19) Khatoon T, Chandel VS, Alam N, Azam A, Srivastava S, Khan S. La3+ substituted Ni0.5 Co0.5 Fe2 O4 nanoferrites: Magnetically separable catalysts for sunlight-driven photo-oxidative degradation of Methylene Blue. *Journal of Alloys and Compounds*. 2023;961. Available from: https://doi.org/10.1016/j.jallcom.2023.171125.